

Direct Evidence of a Dual Cascade in Gravitational Wave Turbulence


Sébastien Galtier^{1,2,3,*} and Sergey V. Nazarenko⁴

¹Laboratoire de Physique des Plasmas, École Polytechnique, F-91128 Palaiseau Cedex, France

²Université Paris-Saclay, IPP, CNRS, Observatoire Paris-Meudon, France

³Institut Universitaire de France

⁴Université Côte d'Azur, CNRS, Institut de Physique de Nice (INPHYNI), Parc Valrose, 06108 Nice, France

 (Received 26 April 2021; revised 10 June 2021; accepted 31 August 2021; published 20 September 2021; corrected 28 February 2022)

We present the first direct numerical simulation of gravitational wave turbulence. General relativity equations are solved numerically in a periodic box with a diagonal metric tensor depending on two space coordinates only, $g_{ij} \equiv g_{ij}(x, y, t)\delta_{ij}$, and with an additional small-scale dissipative term. We limit ourselves to weak gravitational waves and to a freely decaying turbulence. We find that an initial metric excitation at intermediate wave number leads to a dual cascade of energy and wave action. When the direct energy cascade reaches the dissipative scales, a transition is observed in the temporal evolution of energy from a plateau to a power-law decay, while the inverse cascade front continues to propagate toward low wave numbers. The wave number and frequency-wave-number spectra are found to be compatible with the theory of weak wave turbulence and the characteristic timescale of the dual cascade is that expected for four-wave resonant interactions. The simulation reveals that an initially weak gravitational wave turbulence tends to become strong as the inverse cascade of wave action progresses with a selective amplification of the fluctuations g_{11} and g_{22} .

DOI: [10.1103/PhysRevLett.127.131101](https://doi.org/10.1103/PhysRevLett.127.131101)

Introduction.—Wave turbulence (WT) is a state of a continuous medium with random mutually interacting waves of weak amplitude excited over a broad range of wave numbers. The long-time statistical properties of such a medium have a natural asymptotic closure induced by the large separation of linear and nonlinear timescales [1–3]. The dynamics of WT is driven by kinetic equations which describe the redistribution of spectral densities via mainly three- or four-wave resonant interactions. The kinetic equations have two types of exact stationary power-law solutions: the zero-flux equilibrium thermodynamic spectra and the finite flux nonequilibrium Kolmogorov-Zakharov spectra [4]. The latter solutions are much more interesting because they describe the spectral transfer of conserved quantities, such as energy or wave action, generally between a source and a sink [5,6]. The direction of the cascade, direct or inverse, can be found by a numerical evaluation of the sign of the associated flux. The theory also offers the possibility to predict the Kolmogorov constant. All these properties makes WT a very interesting regime to understand the mechanisms underlying turbulence in depth.

WT is of interest to many physical systems for which theoretical predictions have been made and numerically or experimentally verified. We have, among others, capillary waves [7–14] and gravity waves [15–18] on fluid surfaces, inertial waves in rotating hydrodynamics [19–26], elastic waves on thin vibrating plates [27–32], optical waves in optical fibers [33,34], waves in Bose-Einstein condensate

[35,36], Kelvin waves on quantum vortex filaments [37–39], magnetostrophic waves in geodynamo [40,41] and magneto-hydrodynamic waves in space plasmas [42–47]. Recently, a theory of WT has been developed for gravitational waves (GWs) [48], a few years after their first direct detection [49]. A promising application concerns the primordial universe shortly after the hypothetical initial singularity. During this period, GWs can be produced by different mechanisms like, e.g., first order phase transition [50,51] or the merger of primary black holes which can be formed from the primordial space-time fluctuations [52]. A typical length scale of GW excitation can be 10^{-30} m. Following this idea, a scenario of cosmological inflation has been proposed relying on the presence of weak or strong GW turbulence and rapid formation of a condensate via an inverse cascade [53]. In this scenario, the initial strong GW bursts are quickly diluted as they propagate through the surrounding space, resulting in a statistically quasihomogeneous GW field that is weakly or strongly nonlinear depending on the strength and density of forcing events. For the weak WT case, a kinetic equation that describes the dynamics of energy and wave action via four-wave resonant interactions was derived. It has exact stationary scaling solutions for the one-dimensional (1D) isotropic spectrum of wave action: k^{-1} for the direct energy cascade and $k^{-2/3}$ for the inverse wave action cascade. Further, an explosive front propagation in the inverse cascade is predicted and numerically observed with a phenomenological nonlinear diffusion model where strongly

local interactions are retained [54]. With this model, it is also shown that the nonstationary isotropic spectrum of wave action is slightly different from the Kolmogorov-Zakharov solution with a power-law index ~ -0.6517 , instead of $-2/3$ for the stationary solution. However, this regime of WT is realized under assumptions that the initial condition consists of weak waves with random phases, and that the nonlinearity remains weak and the phases remain random during the evolution. Study of validity of such assumptions and robustness of the results with respect to more general (not necessarily wave dominated) initial conditions requires numerical simulations. Besides, the underlying nonlinear dynamics has never been explored in the physical space and this requires the use of numerical simulations.

In this Letter, we report the first direct numerical simulations (DNS) of weak GW turbulence. This regime is studied in both physical and spectral spaces. Our study reveals that, despite having its own distinct properties, space-time turbulence behaves in a classical way from the point of view of the general turbulence theory.

Einstein's equations.—Following [48,55], we shall consider the vacuum general relativity equations [56,57] with the Hadad-Zakharov (2.5 + 1) diagonal metric

$$g_{00} = -(1 + \tilde{\gamma})^2 e^{-2\lambda}, \quad g_{11} = (1 + \tilde{\beta})^2 e^{-2\lambda}, \quad (1)$$

$$g_{22} = (1 + \tilde{\alpha})^2 e^{-2\lambda}, \quad g_{33} = e^{2\lambda}. \quad (2)$$

The metric depends on the space-time variables x , y , and t but is independent of z . It can describe GWs of any amplitude, however, we limit ourselves to weak GW amplitude, i.e., $\tilde{\alpha}, \tilde{\beta}, \tilde{\gamma}, \lambda \ll 1$. Within this limit, Einstein's equations in the leading order are [48]

$$\partial_x \dot{\tilde{\alpha}} = -2\dot{\lambda}(\partial_x \lambda), \quad \partial_y \dot{\tilde{\beta}} = -2\dot{\lambda}(\partial_y \lambda), \quad (3)$$

$$\partial_x \partial_y \tilde{\gamma} = -2(\partial_x \lambda)(\partial_y \lambda), \quad (4)$$

$$\partial_t [(1 + \tilde{\alpha} + \tilde{\beta} - \tilde{\gamma})\dot{\lambda}] = \partial_x [(1 + \tilde{\alpha} - \tilde{\beta} + \tilde{\gamma})\partial_x \lambda] + \partial_y [(1 - \tilde{\alpha} + \tilde{\beta} + \tilde{\gamma})\partial_y \lambda], \quad (5)$$

where we define $\dot{f} \equiv \partial_t f$. The linear solution of this system [see Eq. (5)] is a plus-polarized GW with a dispersion relation $\omega = k$ (with the speed of light $c = 1$ and $k = |\mathbf{k}|$) [58]. For the analysis below, it is useful to recall the link between the canonical variable $a_{\mathbf{k}}$ and the primary variables, $a_{\mathbf{k}} = \sqrt{k/2}\lambda_{\mathbf{k}} + i\sqrt{1/2k}\dot{\lambda}_{\mathbf{k}}$, where $\lambda_{\mathbf{k}}$ is the Fourier transform of λ [48]. The two-dimensional (2D) wave action spectrum will be numerically computed using the relation $N(\mathbf{k}) = |a_{\mathbf{k}}|^2$ (homogeneity will be used as well as plane waves), and the 2D energy spectrum is $E(\mathbf{k}) = \omega N(\mathbf{k})$ [48].

DNS of Eqs. (3)–(5) are performed with an additional dissipative term acting at small scales to avoid numerical instabilities [59]. This term, added in the rhs of Eq. (5), takes the form $-\nu k^4 \lambda_{\mathbf{k}}$ (for $k \geq k_{\text{diss}}$) in Fourier space (see, e.g., [27]). Physically, GW dissipation by matter is

expected through, e.g., Landau damping [60]. (Note that the nondissipative Einstein equations become invalid at the Planck length.) However, in our case, the dissipation has no precise origin and must be considered as a mechanism mimicking existence of a positive energy flux which would, otherwise, be blocked due to the presence of the maximum wave number in our numerical method. We developed a pseudospectral code using FFTW3 routines, with periodic boundary conditions and dealiasing [61]. Since we deal with real fields only, the Fourier space is restricted to $k_y \geq 0$. An Adams-Bashforth numerical scheme is used to integrate the nonlinear terms. For solving the double time derivative in Eq. (5), an intermediate variable $\Lambda = \partial_t \lambda$ is introduced. We also introduce intermediate variables $A = \partial_t \tilde{\alpha}$, $B = \partial_t \tilde{\beta}$, and $G = \partial_t \tilde{\gamma}$ for solving Eqs. (3) and (5) where several time-derivative terms appear. Therefore, in practice, eight equations are numerically solved at each time step ΔT . The simulation shown is made with a spatial resolution of 512 points in each direction, $\nu = 4 \times 10^{-11}$ and $k_{\text{diss}} = 140$. Initially (at $t = 0$), only λ is excited around wave number $k_i = 89$ (in order to see the dual cascade), with random phases, and such that $|\lambda_{\mathbf{k}}|^2 = C(k^2 - 88^2)(90^2 - k^2)$ with $k_{x,y} \in [88, 90]/\sqrt{2}$. The constant C is chosen so that the total wave action is initially equal to 50. The time will be normalized in the linear GW time unit $t_{\text{GW}} = 1/\omega_i = 1/k_i$ (characteristic time of the initial excitation). We take $\Delta T = 10^{-5} t_{\text{GW}}$, which is relatively small but is necessary to avoid numerical instabilities and to ensure the conservation of invariants during the primary phase. The present simulation parameters appear to give the most representative illustration of the processes we study (we have performed a large number of simulations with various values of these parameters).

Results.—Figure 1 shows the global evolution in time, i.e., the root mean square (rms) values, of the basic fields $\tilde{\alpha}$, $\tilde{\beta}$, and λ . We see that $\tilde{\alpha}_{\text{rms}}$ and $\tilde{\beta}_{\text{rms}}$ are strongly correlated with two distinct stages. At the first stage, until $\sim 3500 t_{\text{GW}}$, we see two almost identical signals in which a slight growth is superimposed with oscillations with a typical period of $100 t_{\text{GW}}$. After that, the signals become different from each

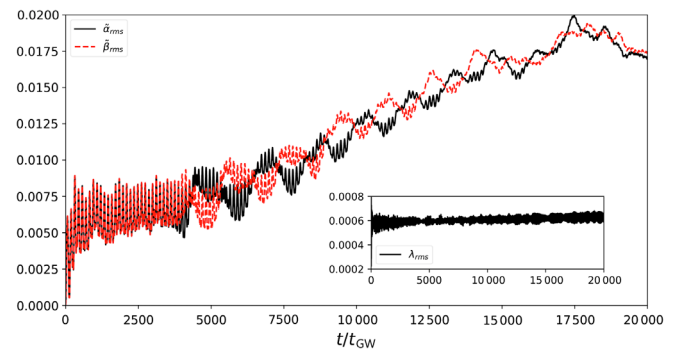


FIG. 1. Time evolution (rms values) of the basic fields $\tilde{\alpha}$, $\tilde{\beta}$, and λ (inset).

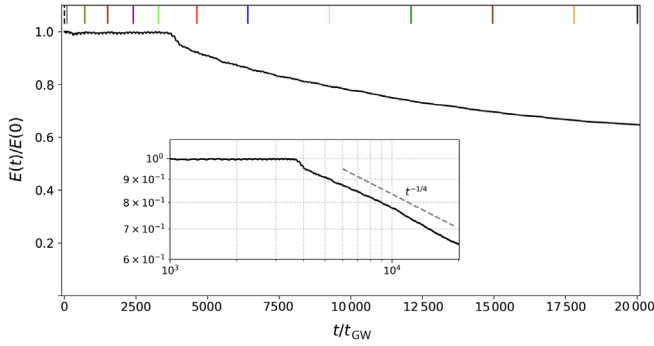


FIG. 2. Time evolution of the normalized energy. Inset: the same variation in log-log reveals a decay close to $t^{-1/4}$. The colored vertical lines at the top correspond to the times chosen to plot the spectra in Fig. 3.

other: the high-frequency oscillations remain, but in addition, there appear long-scale oscillation (with a period about ten times longer) in which $\tilde{\alpha}_{\text{rms}}$ and $\tilde{\beta}_{\text{rms}}$ oscillate in counterphase. At the large scale, both signals increase over time reflecting local amplifications of $\tilde{\alpha}(x, y)$ and $\tilde{\beta}(x, y)$. Overall, $\tilde{\alpha}$ and $\tilde{\beta}$ behave like twin variables with similar dynamics. The behavior of λ_{rms} (shown in the figure inset) and $\tilde{\gamma}_{\text{rms}}$ (not shown) is different with no significant increase in amplitude and faster oscillations with a period close to t_{GW} .

In Fig. 2, we show the temporal evolution of the normalized energy E (with initially $E(t=0) = 28185$). Two phases are clearly present. First, the energy is conserved until $\sim 3500t_{\text{GW}}$. This phase corresponds to the time interval needed to develop a direct energy cascade and to reach the small dissipative scales (see Fig. 3). This observation can be seen as evidence of the accuracy of

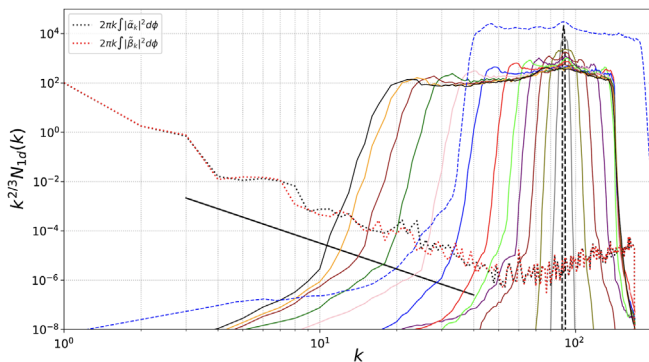


FIG. 3. Time evolution of $k^{2/3}N_{1d}(k)$ (solid lines) with the initial spectrum in black dashed line. Corresponding times are given in Fig. 2. The same spectrum, renormalized in scale and amplitude, is shown for an inviscid simulation at a resolution of 1024 points (blue dashed line). The 1D spectra $2\pi k \int_0^{2\pi} |\tilde{\alpha}_{\mathbf{k}}|^2 d\phi$ and $2\pi k \int_0^{2\pi} |\tilde{\beta}_{\mathbf{k}}|^2 d\phi$ are also shown (dotted lines) at the final time of the simulation (at a resolution of 512 points) and compared with the power law $k^{-3.5}$.

the numerical code (the wave action is also conserved during this phase). Then, the energy slowly decreases. To appreciate this decay law, a log-log plot is given in the inset: this reveals a power law decay in time. This type of behavior is classical in freely decaying (strong or weak) turbulence in the presence of a direct cascade (see, e.g., [62,63]).

The evolution in time of the 1D wave action spectrum $N_{1d}(k) = 2\pi k \int_0^{2\pi} N(\mathbf{k}) d\phi$, where ϕ is the polar angle in the k space, is displayed in Fig. 3. The spectra are compensated by the theoretical prediction $k^{-2/3}$ [48]. The propagation toward small scales is interpreted as a signature of a direct energy cascade. If we come back to Fig. 2, we see that the spectrum shown in light green is close to the end of the plateau: this is the moment when the dissipative scales are reached. Afterward, the small-scale propagation of the spectrum is stopped. On the other hand, the development of the front is interpreted as an inverse cascade of wave action, which could be viewed as a strongly nonequilibrium Bose-Einstein condensation process. We see that beyond $3500t_{\text{GW}}$ (from red curve onward) the inverse cascade is preserved with a further expansion of the inertial range characterized by a bump in the front propagation (see, also, Fig. 4). We can already see the presence of a plateau and conclude that our result is qualitatively in agreement with the theoretical prediction. The 1D spectra $2\pi k \int_0^{2\pi} |\tilde{\alpha}_{\mathbf{k}}|^2 d\phi$ and $2\pi k \int_0^{2\pi} |\tilde{\beta}_{\mathbf{k}}|^2 d\phi$ are shown in dotted lines: as expected, α and β are much smaller than λ [since $N_{1d}(k) \sim k^2 |\lambda_{\mathbf{k}}|^2$] in the inertial range of WT. However, we observe a significant selective amplification of α and β at large scales, which is not described by the weak WT theory. Respectively, it means an amplification of the metric components g_{11} and g_{22} at the large scales while g_{00} and g_{33} remain in fast oscillations only (see, also, Fig. 6). For the GWs, such large-scale variations of g_{11} and g_{22} are perceived as a slow

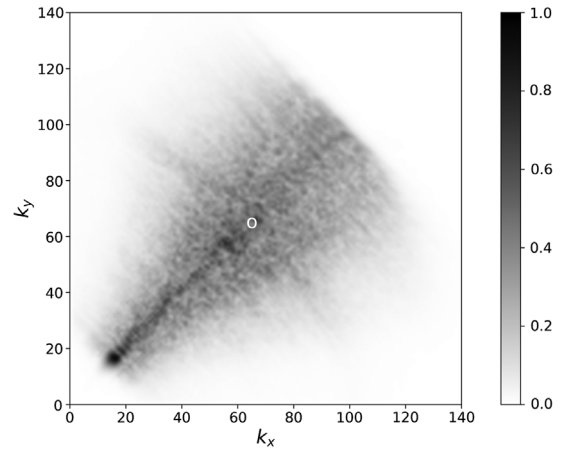


FIG. 4. $N(\mathbf{k})$ around the final time of the simulation (mean over 4 times). The center of the domain of initial excitation is indicated by the symbol “o”.

variation of the scale factor of the underlying space, i.e., its expansions and contractions. Superimposed to these plots, we also show the spectrum of an inviscid (i.e., $\nu = 0$) simulation at 1024 points resolution with an initial excitation at $k_i = 128$ (with same time step and type of initial condition). The simulation is stopped before reaching the smallest scales. The spectrum is renormalized in scale such that the initial excitation is moved to 89. The purpose of this plot is to confirm the dual cascade while we are still in the conservative phase, with a plateau at large scales and, at small scales, a wider inertial range compared to the 512^2 simulation.

In Fig. 4, the normalized 2D wave action spectrum is shown around the final time of the simulation to appreciate the number of modes excited during these cascades. The presence of a bow at large wave numbers can be seen as the signature of the dissipation which starts abruptly at $k = 140$. This plot reveals that a large domain in Fourier space is affected by the cascades which start around the symbol “o.” Note that we are still far from the axes, and no condensation is found. Note, also, a dark spot at the smallest excited wave numbers corresponding to a spectrum amplification. It points out an overshoot nature of the propagating condensation front with a significant localized lump of wave action moving toward the smaller k 's. Also, the 2D spectrum looks like a wedge or angle, which means that the propagation toward the large and the small scales takes place without significant spreading in the angular distribution of the wave propagation, i.e., without a full isotropization.

WT is a state dominated by waves of weak amplitude; all nonwave initial disturbances eventually die out. Such a system is characterized by a very specific ω - k spectrum that concentrates near the dispersion relation curve of the wave in question [17,18,21,23,30,32,39,41,44]. It is also the case for GW turbulence, as we can see in Fig. 5 where a ω - k spectrum is plotted. This plot is obtained by taking the time evolution of the canonical variable $a_{\mathbf{k}}$ (real part) for $t/t_{\text{GW}} \in [17\,000, 20\,000]$. Then, we analyze signals corresponding to $k \in [1, 140]$, such that $k_x = k_y$. A Fourier transform in time is then applied to each signal weighted with a Hamming function. The modulus squared of each signal normalized by its maximum is, then, plotted. We see

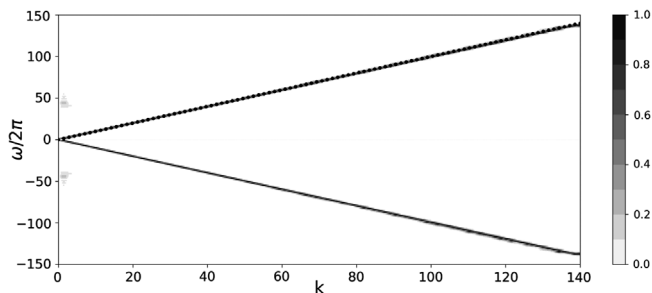


FIG. 5. ω - k spectrum of wave action. The dotted line corresponds to the dispersion relation of a GW.

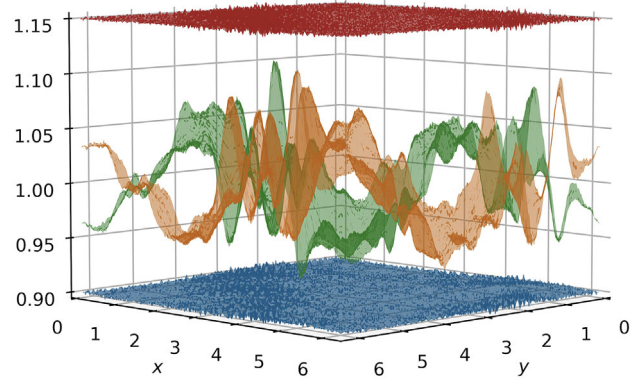


FIG. 6. Metric components g_{00} (blue), g_{11} (orange), g_{22} (green), and g_{33} (red) at the final time of the simulation. g_{00} and g_{33} have been vertically shifted by $+1.9$ and $+0.15$, respectively.

that a signal is obtained along the dispersion relation (dotted line) confirming the wavelike character of this turbulence.

In Fig. 6, the four metric components are plotted at the final time of the simulation. We see that the dominant components are g_{11} and g_{22} whose large-scale oscillations are approximately in antiphase. The two other metric components g_{00} and g_{33} are characterized by relatively small small-scale fluctuations around -1 and $+1$, respectively. These fluctuations remain relatively small during the entire simulation. We have found that g_{11} and g_{22} behave similar to each other during the simulation with, mainly, an anticorrelation and a gradual increase of the fluctuations. This observation is consistent with the behavior observed in Fig. 1, where an increase of $\tilde{\alpha}$ and $\tilde{\beta}$ is also reported. The final time reported, here, is a reasonable limit to stop the simulation because the original equations used (3)–(5) are only valid for weak GWs (which correspond to small fluctuations around ± 1 of the metric components). Interestingly, this final time, $t \sim 10^4 t_{\text{GW}}$, corresponds to the expected time required to develop the weak turbulence regime when the small parameter ϵ used for the expansion is ~ 0.1 : indeed, a phenomenological evaluation gives a typical cascade time $\tau_{\text{cascade}} \sim \epsilon^4 t_{\text{GW}}$ for four-wave interactions (whereas it would be $\sim \epsilon^2 t_{\text{GW}}$ for three-wave interactions) [5]. Note that this is an extremely slow timescale from a numerical point of view that limits us to a relatively low spatial resolution (which, however, proved to be sufficient to obtain physical results, here) [64].

Conclusion.—In this Letter, we have reported the first DNS of GW turbulence. Specifically, the weak regime was studied for which analytical predictions exist. By using both physical and Fourier spaces, we have been able to show that WT can emerge from an initial excitation of the space-time metric with a dual cascade of energy and wave action. This behavior is understood as the result of four-wave resonant interactions of the $2 \leftrightarrow 2$ type for which the wave action is an invariant. Further, we have observed a new effect which is beyond the weak WT predictions—emergence and

continuous amplification of strong large-scale fluctuations of metric components g_{11} and g_{22} while the other components exhibit only weak small-scale oscillations. In particular, the temporal component g_{00} remains close to one which provides a natural cosmic time for weak GW turbulence. The amplification of g_{11} and g_{22} limits our study since, initially, weak WT tends to become strong at large scales [53]. In principle, the regime of strong WT can, then, be studied numerically with the metric (1)–(2) (whose form is preserved at all times as proved by [55]) by including all nonlinear terms of Einstein’s equations.

The main conclusion of this Letter is that it is possible to produce turbulence in general relativity. Unlike the classical hydrodynamic turbulence, it does not consist of randomly interacting vortices but, rather, it takes a form of random interacting waves—the wave turbulence. Further, we show that GW turbulence is a dual cascade system. Namely, in addition to the direct energy cascade, there is an inverse cascade of wave action. The latter is important as it may shed light on the processes in early Universe [53]. We can also mention a strong similarity to elastic wave turbulence in the high tension limit. Indeed, both problems involve four-wave interactions with an inverse cascade of wave action [32]. This similarity could be a motivation to pursue the comparison in an analog laboratory experiment to better understand strong GW turbulence in cosmology and the formation of a metric condensate.

*sebastien.galtier@lpp.polytechnique.fr

- [1] D. Benney and P. Saffman, *Proc. R. Soc. A* **289**, 301 (1966).
- [2] D. Benney, *J. Math. Phys. (N.Y.)* **46**, 115 (1967).
- [3] D. Benney and A. Newell, *J. Math. Phys. (N.Y.)* **46**, 363 (1967).
- [4] V. Zakharov, V. L’Vov, and G. Falkovich, *Kolmogorov Spectra of Turbulence I: Wave Turbulence*, Springer Series in Nonlinear Dynamics (Springer, Berlin, 1992).
- [5] S. Nazarenko, *Wave Turbulence*, Lecture Notes in Physics Vol. 825 (Springer Verlag, Berlin, 2011).
- [6] A. C. Newell and B. Rumpf, *Annu. Rev. Fluid Mech.* **43**, 59 (2011).
- [7] D. J. Benney and A. C. Newell, *Phys. Fluids* **10**, S281 (1967).
- [8] V. Zakharov and N. Filonenko, *J. Appl. Mech. Tech. Phys.* **8**, 37 (1967).
- [9] M. Lommer and M. Levinsen, *J. Fluorescence* **12**, 45 (2002).
- [10] A. Pushkarev and V. Zakharov, *Physica (Amsterdam)* **135D**, 98 (2000).
- [11] M. Y. Brazhnikov, G. Kolmakov, A. Levchenko, and L. Mezhev-Deglin, *JETP Lett.* **73**, 398 (2001).
- [12] L. Deike, D. Fuster, M. Berhanu, and E. Falcon, *Phys. Rev. Lett.* **112**, 234501 (2014).
- [13] Y. Pan and D. K. P. Yue, *Phys. Rev. Lett.* **113**, 094501 (2014).
- [14] M. Berhanu, E. Falcon, G. Michel, C. Gissinger, and S. Fauve, *Europhys. Lett.* **128**, 34001 (2019).
- [15] V. Zakharov and N. Filonenko, *Doclady Akad. Nauk. SSSR* **170**, 1292 (1966).
- [16] É. Falcon, C. Laroche, and S. Fauve, *Phys. Rev. Lett.* **98**, 094503 (2007).
- [17] P. Clark di Leoni, P. J. Cobelli, and P. D. Mininni, *Phys. Rev. E* **89**, 063025 (2014).
- [18] Q. Aubourg and N. Mordant, *Phys. Rev. Lett.* **114**, 144501 (2015).
- [19] S. Galtier, *Phys. Rev. E* **68**, 015301(R) (2003).
- [20] F. Bellet, F. Godefert, J. Scott, and C. Cambon, *J. Fluid Mech.* **562**, 83 (2006).
- [21] E. Yarom and E. Sharon, *Nat. Phys.* **10**, 510 (2014).
- [22] P. Clark di Leoni and P. Mininni, *J. Fluid Mech.* **809**, 821 (2016).
- [23] T. Le Reun, B. Favier, A. J. Barker, and M. Le Bars, *Phys. Rev. Lett.* **119**, 034502 (2017).
- [24] E. Monsalve, M. Brunet, B. Gallet, and P.-P. Cortet, *Phys. Rev. Lett.* **125**, 254502 (2020).
- [25] T. Le Reun, B. Favier, and M. Le Bars, *Europhys. Lett.* **132**, 64002 (2020).
- [26] N. Yokoyama and M. Takaoka, *J. Fluid Mech.* **908**, A17 (2021).
- [27] G. Düring, C. Josserand, and S. Rica, *Phys. Rev. Lett.* **97**, 025503 (2006).
- [28] A. Boudaoud, O. Cadot, B. Odille, and C. Touzé, *Phys. Rev. Lett.* **100**, 234504 (2008).
- [29] N. Mordant, *Phys. Rev. Lett.* **100**, 234505 (2008).
- [30] P. Cobelli, P. Petitjeans, A. Maurel, V. Pagneux, and N. Mordant, *Phys. Rev. Lett.* **103**, 204301 (2009).
- [31] S. Chibbaro and C. Josserand, *Phys. Rev. E* **94**, 011101(R) (2016).
- [32] R. Hassaini, N. Mordant, B. Miquel, G. Krstulovic, and G. Düring, *Phys. Rev. E* **99**, 033002 (2019).
- [33] S. Dyachenko, A. Newell, A. Pushkarev, and V. Zakharov, *Physica (Amsterdam)* **57D**, 96 (1992).
- [34] J. Laurie, U. Bortolozzo, S. Nazarenko, and S. Residori, *Phys. Rep.* **514**, 121 (2012).
- [35] S. Nazarenko, *JETP Lett.* **83**, 198 (2006).
- [36] D. Proment, S. Nazarenko, and M. Onorato, *Physica (Amsterdam)* **241D**, 304 (2012).
- [37] D. Kivotides, J. C. Vassilicos, D. C. Samuels, and C. F. Barenghi, *Phys. Rev. Lett.* **86**, 3080 (2001).
- [38] E. Kozik and B. Svistunov, *Phys. Rev. Lett.* **92**, 035301 (2004).
- [39] S. Nazarenko and M. Onorato, *Physica (Amsterdam)* **219D**, 1 (2006).
- [40] S. Galtier, *J. Fluid Mech.* **757**, 114 (2014).
- [41] N. Bell and S. Nazarenko, *J. Phys. A* **52**, 445501 (2019).
- [42] S. Galtier, S. Nazarenko, A. Newell, and A. Pouquet, *J. Plasma Phys.* **63**, 447 (2000).
- [43] S. Galtier, *J. Plasma Phys.* **72**, 721 (2006).
- [44] R. Meyrand, K. Kiyani, and S. Galtier, *J. Fluid Mech.* **770**, R1 (2015).
- [45] R. Meyrand, S. Galtier, and K. H. Kiyani, *Phys. Rev. Lett.* **116**, 105002 (2016).
- [46] R. Meyrand, K. H. Kiyani, Ö. D. Gürçan, and S. Galtier, *Phys. Rev. X* **8**, 031066 (2018).
- [47] V. David and S. Galtier, *Astrophys. J. Lett.* **880**, L10 (2019).
- [48] S. Galtier and S. V. Nazarenko, *Phys. Rev. Lett.* **119**, 221101 (2017).

- [49] B. Abbott *et al.*, *Phys. Rev. Lett.* **116**, 061102 (2016).
- [50] E. Witten, *Phys. Rev. D* **30**, 272 (1984).
- [51] L. M. Krauss, *Phys. Lett. B* **284**, 229 (1992).
- [52] B. Carr, F. Kühnel, and M. Sandstad, *Phys. Rev. D* **94**, 083504 (2016).
- [53] S. Galtier, J. Laurie, and S. Nazarenko, *Universe* **6**, 98 (2020).
- [54] S. Galtier, S. V. Nazarenko, E. Buchlin, and S. Thalabard, *Physica (Amsterdam)* **390D**, 84 (2019).
- [55] Y. Hadad and V. Zakharov, *J. Geom. Phys.* **80**, 37 (2014).
- [56] A. Einstein and K. Sitzungsber, *Preuss. Akad. Wiss. (Berlin)*, Seite 844 (1915).
- [57] A. Einstein and K. Sitzungsber, *Preuss. Akad. Wiss. (Berlin)*, Seite 688 (1916).
- [58] M. Maggiore, *Gravitational Waves, Volume 1* (Oxford University Press, New York, 2008).
- [59] F. Pretorius, *Phys. Rev. Lett.* **95**, 121101 (2005).
- [60] G. Baym, S. P. Patil, and C. J. Pethick, *Phys. Rev. D* **96**, 084033 (2017).
- [61] V. Shukla, P. D. Mininni, G. Krstulovic, P. C. di Leoni, and M. E. Brachet, *Phys. Rev. A* **99**, 043605 (2019).
- [62] S. Galtier, H. Politano, and A. Pouquet, *Phys. Rev. Lett.* **79**, 2807 (1997).
- [63] B. Bigot, S. Galtier, and H. Politano, *Phys. Rev. Lett.* **100**, 074502 (2008).
- [64] A run at resolution 1024^2 takes about six months.

Correction: The fourth affiliation was presented incorrectly and has been fixed.